

## Fracture toughness measurements on bovine enamel by indentation techniques

**J. Rodríguez<sup>1\*</sup>, M.A. Garrido<sup>1</sup>, L. Ceballos<sup>2</sup>**

<sup>1</sup> Departamento de Tecnología Mecánica, Universidad Rey Juan Carlos, 28933 Madrid, Spain

<sup>2</sup> Departamento de Estomatología, Universidad Rey Juan Carlos, 28933 Madrid, Spain

\* Corresponding author: [jesus.rodriquez.perez@urjc.es](mailto:jesus.rodriquez.perez@urjc.es)

---

**Abstract.** Many works have attempted to estimate the fracture toughness of enamel by indentation techniques. Most of these works have in common the use of equations whose success in determining the actual value of fracture toughness depends on the particular three-dimensional pattern of cracks. Although microscopic techniques are usually employed, only a superficial image of the cracks is provided, and no information about the propagation within the enamel is given. Therefore, there is some uncertainty about the applicability of this type of equations. More recently, an alternative methodology based on an energetic approach has been developed to estimate the fracture toughness by depth sensing indentation that is not so affected by the cracks pattern generated.

In this work, the energetic approach to indentation fracture toughness of bovine enamel is presented and compared with those toughness values obtained using the most common expressions reported in the literature. The results showed that some modifications in the energetic methodology should be performed in order to apply it successfully.

**Keywords** indentation fracture toughness, enamel

---

### 1. Introduction

Enamel is the hardest and stiffest tissue of mammals. It forms the outer layer of the tooth and shows a characteristic hierarchical microstructure. At large scale, the enamel consists of rods encapsulated by thin protein rich sheaths that are arranged parallel in a direction perpendicular to the dentino-enamel junction (DEJ) from dentin to the outer enamel surface [1]. The enamel microstructure of all mammals appears to be very similar on a histochemical and anatomic basis [2].

Numerous methods have been employed to experimentally measure the fracture toughness ( $K_C$ ) of the enamel. The determination of  $K_C$  by indentation technique is based on measuring the size of cracks induced in a material during indentation. Several expressions are available to determine  $K_C$  by this technique, depending on the indenter geometry and crack morphology. One of the most widely used expressions for radial cracks is the relationship proposed by Lawn, Evans and Marshall [3]:

$$K_C = k \left( \frac{E}{H} \right)^n \frac{P}{c^{3/2}} \quad (1)$$

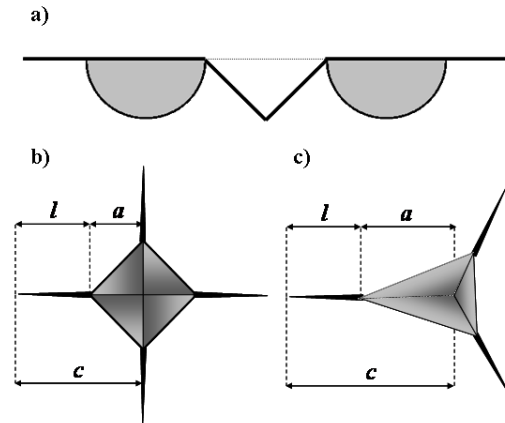


Figure 1. a) Palmqvist cracks configuration; b) crack parameters for Vickers indenter; c) crack parameters for Berkovich indenter.

where  $P$  is the maximum indentation load,  $c$  is the crack length (Fig. 1),  $E$  is the elastic modulus and  $H$  is the hardness. The parameters  $k$  and  $n$  are empirical constants equal to  $0.016 \pm 0.004$  and  $0.5$ , respectively. Other studies [4] determined  $k = 0.0098$  and  $n = 3/2$ .

For Palmqvist cracks configuration, where the cracked areas are represented by semicircles of diameter equal to the crack length measured from an impression corner (Fig. 1a), many expressions have been developed to calculate  $K_C$ . Niihara et al. [5] proposed the following expression:

$$K_C = k \left( \frac{E}{H} \right)^{2/5} \frac{P}{a\sqrt{l}} \quad (2)$$

where  $a$  is the half-diagonal of the indentation impression,  $l$  is the crack length and  $k$  was determined as  $0.0089$  (Fig. 1b).

Laugier [6] proposed an alternative expression for Palmqvist cracks:

$$K_C = x_V \left( \frac{a}{l} \right)^{1/2} \left( \frac{E}{H} \right)^{2/3} \frac{P}{c^{3/2}} \quad (3)$$

where  $x_V$  was determined as  $0.015$ .

However, the applicability of these equations encounters three basic difficulties. First, all these equations are semi-empirical as there is no theoretical basis behind these expressions. Second, it is necessary to obtain a particular pattern of cracks (Fig. 1a) and to know the morphology of the cracks in the plane parallel to the loading direction in order to implement the Eqs. (1)-(3). Third, all these equations were developed for ceramic materials and for the symmetrical Vickers indentations (Fig. 1b). Therefore, they are not valid for the asymmetrical Berkovich indentations. Some efforts have been made to obtain similar equations to those described above but properly modified for Berkovich indentations [7] (Fig. 1c). Combining the model proposed by Laugier [6] and the Ouchterlony's radial cracking modification factors [8], fracture toughness can be determined according to Eq. (4).

$$K_C = 1.073 \cdot x_v \left( \frac{a}{l} \right)^{1/2} \left( \frac{E}{H} \right)^{2/3} \frac{P}{c^{3/2}} \quad (4)$$

Other alternative method to determine the fracture toughness consists on calculating the energy released during cracking, as a measure of the fracture toughness (Li et al. 1997) [9]. This method is based on the formation of a constant force step during the application of indentation load. This force step is associated with the sudden formation and propagation of cracks. The step length depends on how much the indenter and cracks suddenly advance into the material. This energetic method calculates the fracture toughness comparing the area limiting by the load-displacement curve with crack generation and the hypothetical one if cracking does not occur (Fig. 2). If the Mode I fracture is assumed, the threshold stress intensity required for the fracture can be written as:

$$K_{IC} = \left[ \left( \frac{E}{(1-\nu^2)} \right) \cdot \left( \frac{\Delta U}{A} \right) \right]^{1/2} \quad (5)$$

where  $K_{IC}$  is the indentation fracture toughness of the material,  $\Delta U$  is the strain energy obtained from the area between extrapolated load-displacement curve and the step of experimental one (Fig. 2),  $E$  is the elastic modulus,  $\nu$  is the Poisson's ratio and  $A$  represents the cracked area.

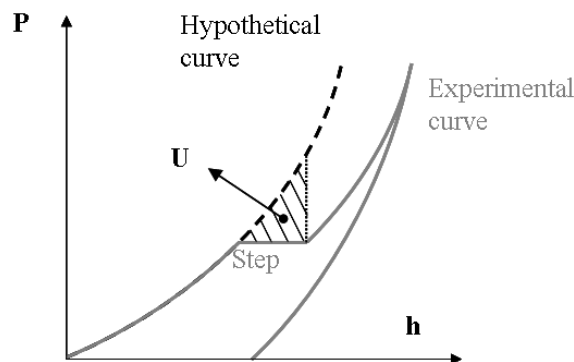


Figure 2. Strain energy obtained from the area between extrapolated load-displacement curve and the step of experimental one.

This method can be used even when a particular cracks pattern is not obtained. However, a constant load step during the loading branch is necessary in order to apply the Eq. (5). Additionally, a good estimation of cracked area is essential to obtain reliable results.

Therefore, the aim of this study was to evaluate the reliability of the energetic methodology using depth sensing indentation technique to estimate the indentation fracture toughness of bovine dental enamel. These values were compared with those traditionally obtained by applying the semi-empirical equations based in a specific pattern of cracks, Eqs. (1)-(4).

## 2. Experimental procedure

Eight incisors were extracted from bovines of two years old. The teeth were cleaned and stored in artificial saliva prior to the tests. The labial surfaces of the specimens were polished using a

mechanical grinder (Labopol-5, Struers, Copenhagen, Denmark) with polishing cloths with alumina suspension slurry of 3  $\mu\text{m}$  and OP-A (Struers, Copenhagen, Denmark). Afterwards, the specimens were kept fully hydrated in artificial saliva at room temperature before the indentation tests.

Hardness and elastic modulus of bovine enamel surfaces were studied by nanoindentation (Nanoindenter XP-MTS System Corporation) using a Berkovich indenter with a tip radius of 100 nm. Before each batch tests, the Berkovich diamond indenter was calibrated on a standard fused silica specimen.

A Continuous Stiffness Measurement module (CSM) was chosen. This method consists of applying multiple unloading cycles of very small displacement during the loading process. The Oliver-Pharr methodology [10] was applied on each of these partial unloading cycles, providing values of elastic modulus,  $E$ , and hardness,  $H$ , as a continuous function of load or penetration depth. A maximum penetration depth of 300 nm was fixed for all indentation tests. Three rows of 20 indentations were done on each sample. Each indentation was separated 100  $\mu\text{m}$  to each other. During the loading branch, continuous loading-unloading cycles with amplitude of 2 nm and a frequency of 45 Hz were superimposed.

Additionally, 5 indentations were done on each sample using the CSM module up to a maximum penetration depth of 2000 nm. This penetration depth was sufficient to generate a characteristic pattern of cracks, which extended from the corners of the Berkovich imprint and propagated along the enamel microstructure. After the indentation tests, the residual imprints were observed by Scanning Electron Microscopy (SEM) under low vacuum condition and taking care that the samples remained inside the microscope the shortest time in order to prevent an excessive dehydration and consequently, the cracks propagation due to residual stresses.

### 3. Results

Figure. 3 shows two SEM images of typical residual imprints from depth sensing indentations at different maximum penetration depths and their corresponding contact stiffness versus contact depth curves: 300 nm (Fig. 3a) and 2000 nm (Fig. 3b). Indentations at maximum penetration depth of 300 nm were characterized by the absence of cracks in the edges of the residual imprint (Fig. 3a). Additionally, the contact stiffness,  $S$ , showed a linear trend with the square root of the contact area,  $A$ , between the indenter and the material surface (Fig. 3a), as predict the theoretical relation between them [10]. By contrast, the indentations obtained for a maximum penetration depth of 2000 nm were characterized by the presence of radial cracks from the edges of the residual imprints (Fig. 3b). All residual imprints showed a similar superficial cracks pattern, consequently, the semi-empirical equations described in the introduction section could be applied. In addition, in these indentation tests, the cracks deflected during their propagation through the enamel microstructure. It was also noted that the contact stiffness lost its linear dependency with the square root of contact area (Fig. 3b), coinciding with the formation and propagation of cracks during the indentation process.

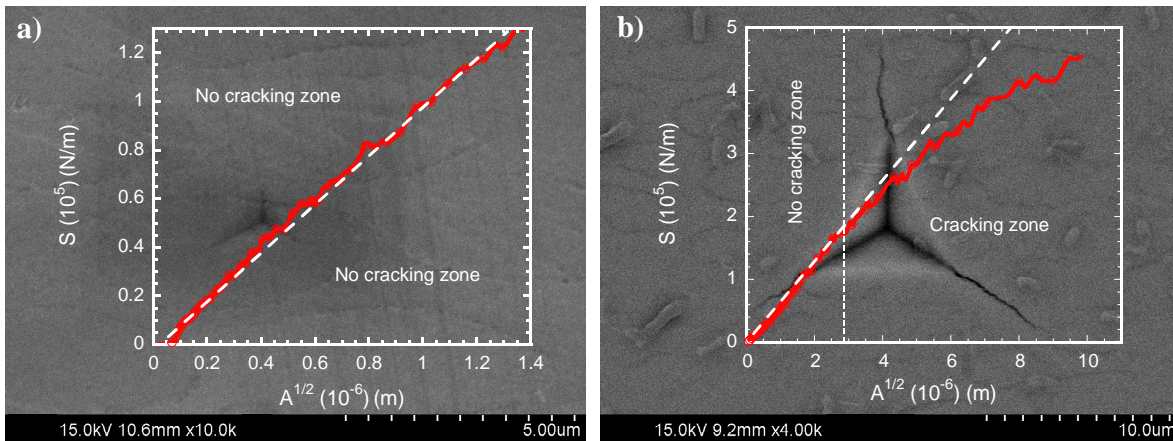


Figure 3. Typical pattern of cracks obtained from nanoindentations carried out at different maximum penetration depths: a) 300 nm; b) 2000 nm. Their corresponding indentation contact stiffness versus squared root of the contact area plots were put over each image.

### 3.1. Mechanical properties: elastic modulus, hardness and fracture toughness.

Table 1 summarizes the hardness and elastic modulus of bovine enamel obtained from indentation tests at maximum penetration depth of 300 nm, where the loading did not cause the initiation of cracks. The values obtained in this study were very similar to those reported in previous works [11-13].

Data in Table 1 also include the fracture toughness of enamel according to the equations previously described (see Eqs. (1-5)).

It is noteworthy that, in all cases, there was not any constant load step. Therefore, it was not possible to apply the energetic methodology as described in the introduction section.

<b>Elastic modulus, <math>E</math> (GPa)</b>	$92 \pm 6$	Oliver-Pharr [10]
<b>Hardness, <math>H</math> (GPa)</b>	$4.7 \pm 0.3$	Oliver-Pharr [10]
<b>Indentation fracture toughness, <math>K_C</math> (<math>\text{MPa}\sqrt{\text{m}}</math>)</b>	$0.39 \pm 0.14$	Eq (1) [3]
	$0.5 \pm 0.2$	Eq (2) [5]
	$0.6 \pm 0.2$	Eq (3) [6]
	$0.7 \pm 0.2$	Eq (4) [8]
	$2.5 \pm 0.7$	Eq (9)

Table 1. Experimental results of elastic modulus,  $E$ , hardness,  $H$  and indentation fracture toughness,  $K_C$ .

## 4. Discussion

There is some scatter in the literature about the actual fracture toughness of enamel [13]. Table 1 shows the fracture toughness values obtained after applying the semi-empirical equations (1) to (4). These data were within the range of those reported by other authors. Hassan et al. (1981) [14] have reported values of human tooth enamel, using a Vickers indenter combined with a semi-empirical equation type 1 (Eq. (1)), in the range of 0.7 to 1.37 MPa·m<sup>1/2</sup>. Xu et al. (1998) [12] reported fracture toughness values of 0.84 MPa·m<sup>1/2</sup> for labial human enamel also using a Vickers indenter with semi-empirical equation type 1 (Eq. (1)). Bajaj and Arola (2009) [15] reported fracture toughness values for human enamel that ranged from 1.79 MPa·m<sup>1/2</sup> to 2.37 MPa·m<sup>1/2</sup> obtained from R-curve analysis, and Baldassarri et al. (2008) [16] obtained values of 0.5 MPa·m<sup>1/2</sup> and 1.3 MPa·m<sup>1/2</sup> for transversal and midsagittal enamel orientation, respectively, using a Vickers indenter on rat tooth. Rasmussen and Patchin (1984) [17] used SEM fractography and work-of-fracture techniques to investigate the fracture properties of human enamel and dentin as a function of the temperature of an aqueous environment. In this work, the specimens were notched in order to give controlled fracture in one of two preferred directions, either "perpendicular" or "parallel" to the rods for enamel. They reported values of work-of-fracture for human enamel that range from 0.13 J/m<sup>2</sup> (fracture toughness of 1.09 MPa·m<sup>1/2</sup>) for parallel direction to 1.90-2.00 J/m<sup>2</sup> (fracture toughness of 4.18-4.29 MPa·m<sup>1/2</sup>) for perpendicular orientation, at room temperature. The experimental load-displacement curves did not show, in our case, a constant load step during the loading branch (Fig. 5). In order to apply an energetic approach, an alternative methodology had to be developed.

The proposed procedure is based on the contact stiffness variation due to cracking during the indentation process. It should be noted that besides the cracking process, could also have other phenomena that may affect the contact stiffness, as quasi-plastic deformation phenomena associated with the movement of the water and protein phase due to the indentation. However, given the conditions under which the indentation tests were made, with high frequencies of the loading and unloading cycles (45 Hz), and small penetration depths in each cycle (2 nm), the contribution of these phenomena to the variation of the contact stiffness can be considered negligible.

It is well known that the area under the load-displacement curve is the work performed by the indenter during elastic-plastic deformation. However, if cracking occurs, part of the elastic energy stored will be released to create new crack surfaces. This will be reflected as a change in the contact stiffness and, consequently, the relationship between contact stiffness,  $S$ , and the squared root of the contact area,  $A$ , will not be linear as the contact theory predicts [10]:

$$S = 2 \cdot E_r \cdot \frac{\sqrt{A}}{\sqrt{\pi}} \quad (6)$$

where  $E_r$  is the reduced elastic modulus. For Berkovich indenters, the contact area is obtained from the following equation:

$$A = 24.5 \cdot h_p^2 + C_1 \cdot h_p + C_2 \cdot h_p^{1/2} + C_3 \cdot h_p^{1/4} + \dots \quad (7)$$

where  $h_p$  is the contact depth and  $C_i$  are fitting constants obtained from calibration on fused silica.

As Fig. 3 showed, in a typical curve of contact stiffness versus squared root of the contact area, the tendency should be linear according to Eq. (6); however, the linearity only remains during the initial stage, before cracking occurs.

It is possible to identify in the  $S-A^{1/2}$  curve a critical point associated with the onset of cracking ( $S^*$ ,  $A^{1/2*}$ ). To do this, successive linear fits were made until a minimum regression coefficient of 0.99 was reached.

According to the Oliver-Pharr methodology [10], it is possible to calculate the load and penetration depth values corresponding to the critical point associated with the cracking initiation,  $P^*$  and  $h^*$ .

For values ( $P$ ,  $h$ ) lower than the critical point, the indentation process took place without cracking. For higher values, the indentation process was characterized by the nucleation and propagation of cracks. The load-penetration depth curve for values lower than the critical one was extrapolated according to the Kick's law [18],  $P=C \cdot h^2$ , to the maximum penetration depth of 2000 nm, obtaining a hypothetical curve characteristic of a non cracking process. Fig. 4 shows a comparative example between the experimental indentation curve, with cracking and the hypothetical indentation curve without cracking.

Now, it is possible to apply the energetic methodology through Eq. (5) with the consideration that the strain energy associated to the cracking process,  $\Delta U$ , could be obtained from the difference between the hypothetical and experimental indentation curves up to the maximum penetration depth, when the maximum crack length was reached. The indentation fracture toughness values so obtained are included in Table 2.

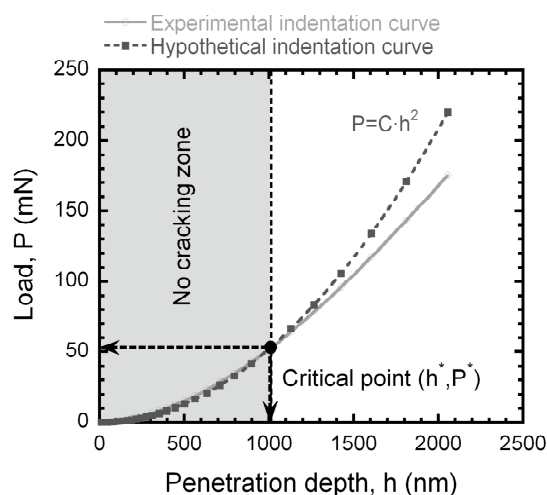


Figure 4. Indentation load versus penetration depth of experimental and hypothetical indentation curve.

## 5. Conclusions

In this work, an energetic methodology, adapted to depth sensing indentation, has been developed to determine the enamel fracture toughness. The method is based on the contact stiffness variation due to the cracking process. The values obtained using this methodology, were compared with those provided by traditional equations based on a particular crack pattern. The results obtained were in agreement with those reported by other authors that use traditional tests to evaluate the fracture toughness of the enamel.

## References

- [1] Von Koenigswald, W., Sander, P.M., 1997. Tooth Enamel Microstructure. Von Koenigswald, W., Sander, P.M., editors. Taylor & Francis publisher. 37-41 Mortimer Street, London, W1T 3JH.
- [2] Eisenmann, D.R., 1998. Enamel structure. In: Oral Histology. Development, Structure and Function. AR Ten Cate editor. St. Louis, pp. 218-235.
- [3] Lawn, B.R., Evans, A.G., Marshall, D.B., 1980. Elastic/plastic indentation damage in ceramics: The median/radial crack system. *J. Am. Ceram. Soc.* 63, 574–581.
- [4] Anstis, G.R., Chantikul, P., Lawn, B.R., Marshall, D.B., 1981. A Critical Evaluation of Indentation Techniques for measuring Fracture Toughness: I, Direct Crack Measurements. *J. Am. Ceram. Soc.* 64, 533-538.
- [5] Niihara, K., Morena, R., Hasselmann, D.P.H., 1983. A fracture mechanics analysis of indentation-induced Palmqvist crack in ceramics. *J. Mater. Sci. Lett.* 2, 221-223.
- [6] Laugier, M.T., 1987. New formula for indentation toughness in ceramics. *J. Mater. Sci. Lett.* 6, 355–356.
- [7] Mullins, L.P., Bruzzi, M.S., McHugh, P.E., 2007. Measurement of the microstructural fracture toughness of cortical bone using indentation fracture. *J. Biomech.* 40, 3285–3288.
- [8] Ouchterlony, F., 1976. Stress intensity factors for the expansion loaded star crack. *Eng. Fract. Mech.* 8, 447-448.
- [9] Li, X., Diao, D., Bhushan, B., 1997. Fracture mechanisms of thin amorphous carbon films in nanoindentation. *Acta Mater.* 45, 4453-4461.
- [10] Oliver, W.C., Pharr, G.M., 1992. An improved technique for determining hardness and elastic modulus using load and displacement sensing indentation experiments. *J. Mater. Res.* 7, 1564-1583.
- [11] Garrido, M.A., Giráldez, I., Ceballos, L., Gómez del Río, M.T., Rodríguez, J., 2011. Nanotribological behaviour of tooth enamel rod affected by bleaching treatment. *Wear.* 271, 2334– 2339.
- [12] Xu, H.H.K., Smith, D.T., Jahanmir, S., Romberg, E., Kelly, J.R., Thompson, V.P., Rekow, E.D., 1998. Indentation damage and mechanical properties of human enamel and dentin. *J.*

Dent. Res. 77, 472–480.

- [13] He, L.H., Swain, M.V., 2008. Understanding the mechanical behavior of human enamel from its structural and compositional characteristics. *J. Mech. Behav. Biomed. Mater.* 1, 18-29.
- [14] Hassan, R., Caputo, A.A., Bunshash, R.F., 1981. Fracture toughness of human enamel. *J. Dent. Res.* 60, 820-827.
- [15] Bajaj, D., Arola, D., 2009. On the R-curve behavior of human tooth enamel. *Biomater.* 30, 4037-4046.
- [16] Baldassarri, M., Margolis, H.C., Beniash, E., 2008. Compositional Determinants of Mechanical Properties of Enamel. *J. Dent. Res.* 87, 645-649.
- [17] Rasmussen, S.T., Patchin, R.E., 1984. Fracture Properties of Human Enamel and Dentin in an Aqueous Environment. *J. Dent. Res.* 63, 1362-1368.
- [18] Kick, F., 1885. *Das Gesetz der proportionalen Widerstande und seine Anwendung*, Art. Felix, Leipzig.